

Multiparticle production in small- x deep inelastic scattering and the nature of the Pomeron

A. Capella, A. Kaidalov, V. Neichitailo and J. Tran Thanh Van

Laboratoire de Physique Théorique et Hautes Energies¹

Université de Paris XI, Bâtiment 210, F-91405 Orsay Cedex, France

Abstract

Properties of multiparticle final states produced in the central rapidity region of small- x deep inelastic scattering (DIS) are discussed. It is pointed out that these properties contain important information on the nature of the Pomeron - used for the description of $\sigma_{\gamma^*P}^{(tot)}$ and diffractive production in DIS. It is shown that models based on universality of the Pomeron predict charged particle multiplicities in small- x DIS which are in good agreement with recent HERA results.

LPTHE Orsay 97-58

November 1997

¹Laboratoire associé au Centre National de la Recherche Scientifique - URA D0063

1 Introduction

Small- x DIS provides a good testing ground for theoretical approaches to high-energy interactions of photons and hadrons. A strong increase of the structure function of the proton $F_2(x, Q^2)$ as x decreases observed at HERA [1, 2] has been often considered as an indication of the existence of the “hard” Pomeron, predicted by QCD-perturbation theory [3, 4]. On the other hand models based on the standard perturbative QCD-evolution provide a good description of experimental data [5]-[8]. However, these two approaches do not explain the striking difference between the energy dependence of total cross sections for hadronic (or γp) interactions and γ^*p -interactions observed experimentally. In ref. [9] a unified approach to hp , γp interactions and DIS has been proposed, where the Pomeron pole is assumed to be universal, i.e. the same in soft and hard processes, with an intercept $\alpha_P(0) \approx 1.2$. The non-universality of the energy behaviour for $hp(\gamma p)$ and γ^*p -interactions is attributed to the different sizes of unitarity corrections (multipomeron exchanges) in these two classes of processes. It was argued that in DIS the unitarization corrections due to multipomeron exchange are much smaller than in hadronic interactions. In the latter the unitarity corrections reduce the effective Pomeron intercept from $\alpha_P(0) \approx 1.2$ to roughly 1.1. On the contrary, in DIS the “bare” intercept $\alpha_P(0) = 1.2$ is only slightly modified by the unitary corrections and provides a “singular” ($F_2(x, Q^2) \sim x^{-0.2}$) initial condition for perturbative QCD evolution. The change between an effective intercept of about 1.1 and the bare one of 1.2 occurs very quickly when Q^2 increases from zero (at $Q^2 \gtrsim 1 \text{ GeV}^2$ the effective intercept is already quite close to the bare one).

A study of structure functions of the proton can hardly discriminate between different theoretical approaches. Investigation of diffractive production of hadrons by real and virtual photons provides extra tests of different theoretical models.

Here we would like to point out that the properties of multiparticle production in DIS are related to the nature of the Pomeron and can be used to test theoretical models. The same situation takes place in high-energy hadronic interactions. A study of only $\sigma_{hp}^{(tot)}(s)$ and $d\sigma_{hp}^{(el)}(s, t)/dt$ does not allow to discriminate between models with large unitarization effects [12, 13] and models where these effects are small [14]. However a fast increase with energy of charged particle densities in

the central rapidity region, broad multiplicity distributions and long-range rapidity correlations observed in hadronic interactions clearly demonstrate the importance of effects related to the multipomeron exchanges [12] [15].

We shall demonstrate below that the model based on universality of the Pomeron, discussed above, gives parameter free predictions for charged particle densities and multiplicities in the central rapidity region of DIS. These predictions are in a good agreement with HERA experimental data [16].

2 Description of the model

The CKMT-model [9] for small- x DIS corresponds to the diagrams for elastic γ^*p -amplitude, shown in Fig. 1, where the upper blobs denote all diagrams which describe the coupling of the Pomeron to virtual photons. They contain in particular diagrams corresponding to QCD-evolution. Asymptotically (i.e. for $Y \equiv \ell n \frac{W^2}{s_0} \rightarrow \infty$), at fixed Q^2 , the Pomeron amplitude increases as $\exp(\Delta y)$ (where $\Delta = \alpha_P(0) - 1$) with increasing energy, while the blobs in Fig. 1 have finite widths in rapidity. The s -channel cutting of the diagrams of Fig. 1 corresponds to the natural physical picture of γ^*P inelastic interaction [17], shown schematically in Fig. 2. It illustrates the fact that a highly virtual photon produces a cascade of partons with virtualities decreasing along the chain. Systems of partons with small virtuality (of large size) interact strongly with the proton either inelastically (Fig. 2a) or diffractively (Fig. 2b). This picture is similar to the models of Bjorken [18] and Büchmüller [19]. The inelastic production amplitude in Fig. 2a can be expressed as a sum of inelastic cuttings of a single Pomeron diagram (Fig. 1a), two Pomeron exchange diagram (Fig. 1b), etc. Some of these cuttings are shown in Figures 3.

In the models based on the $1/N$ -expansion, the Pomeron corresponds to diagrams for elastic scattering with the topology of a cylinder. The cutting of Fig. 3a leads to a 2-chains configuration as shown in Fig. 4a and that of Fig. 3c to the 4-chains configuration of Fig. 4b.

The weights with which different configurations contribute to the multiparticle production are given by AGK-cutting rules [20] and thus can be fixed if the relative contributions of rescatterings in Fig. 1 are known.

It was already mentioned above that contributions of rescatterings in DIS are much smaller than in hadronic interactions and in first approximation, at available energies, it is possible to consider only the PP -contribution. In this case, the latter contribution can be determined from HERA data on large rapidity-gap events [21, 22]. The ratio of the second rescattering (PP -exchange) to P -exchange is equal (with minus sign) to F_2^D/F_2 (where F_2^D is the diffractive contribution to F_2), which is equal to $10 \div 15$ % in the region $10^{-4} < x < 10^{-2}$ and $2 \text{ GeV}^2 \lesssim Q^2 \lesssim 10^2 \text{ GeV}^2$. For hadronic and γp interactions, this ratio is substantially larger.

It is known that particular multiparticle configurations are more sensitive to contributions of rescatterings than the total cross section. For example the shadowing contribution to the cutting of a single Pomeron shown in Fig. 3b is four times larger than the contribution of the diagram of Fig. 1b [20]. For a study of multiparticle production in DIS we will assume a definite model for the series of rescatterings shown in Fig. 1. An adequate description of hadronic interactions was obtained in the “quasi-eikonal” model [23]. It is the simplest generalization of the eikonal model which allows one to calculate all rescatterings in terms of the double rescattering term. So we shall apply the same model to DIS.

In this model the total cross section $\sigma_{\gamma^*p}(W^2, Q^2)$ can be written in the form [24]

$$\sigma_{\gamma^*p}^{(tot)}(W^2, Q^2) = \sum_{k=0}^{\infty} \sigma_{\gamma p}^k(W^2, Q^2) = \sigma_P(W^2, Q^2) f\left(\frac{Z}{2}\right) \quad (1)$$

where k is the number of cut Pomerons ($k = 0$ corresponds to diffractive production). The contribution of the single Pomeron exchange to $\sigma_{\gamma^*p}^{(tot)}$ is denoted by $\sigma_P(W^2, Q^2) = g(Q^2) \exp(\Delta\xi)$ with $\Delta \equiv \alpha_P(0) - 1$ and $\xi \equiv \ell n \frac{W^2}{Q^2} = \ell n \frac{1}{x}$. Here we have neglected the real part of the Pomeron amplitude - which has a small effect on multiparticle production. The function $f(Z)$, defined as

$$f(Z) = \sum_{n=1}^{\infty} \frac{(-Z)^{n-1}}{n \cdot n!} \quad , \quad (2)$$

takes into account all rescatterings in terms of only one function $Z = \frac{C(Q^2)}{R^2 + \alpha'_P \xi} \exp(\Delta\xi)$. The function Z can be determined from the data on the diffractive cross section

$$\sigma_{\gamma^*p}^0 = \sigma_P(W^2, Q^2) \left[f\left(\frac{Z}{2}\right) - f(Z) \right] \quad (3)$$

or, more precisely, from the ratio

$$R^D \equiv \frac{\sigma_{\gamma^*p}^0}{\sigma_{\gamma^*p}^{(tot)}} = \frac{F_2^D(x, Q^2)}{F_2(x, Q^2)} = \left[1 - \frac{f(Z)}{f\left(\frac{Z}{2}\right)} \right] \quad . \quad (4)$$

The quantity $(R^2 + \alpha'_P \xi)$ in Z is related to the t -dependence of the diffractive production amplitude with $R^2 = 2.2 \text{ GeV}^{-2}$ and $\alpha'_P = 0.25 \text{ GeV}^{-2}$ [9].

The cross sections with k -cut Pomerons (corresponding to final configurations with $2k$ -chains) have the following form [24]

$$\sigma_{\gamma^*p}^k(W^2, Q^2) = \frac{\sigma_P}{kZ} \left[1 - \exp(-Z) \sum_{i=0}^{k-1} \frac{Z^i}{i!} \right] \quad , \quad i \geq 1 \quad . \quad (5)$$

It follows from eqs. (2)-(4) that for small values of the ratio R^D one has $Z \approx 8 \cdot R^D$. Experiments on diffraction dissociation at HERA show that the ratio R^D is practically Q^2 -independent and we shall consider $C(Q^2)$ as a constant in future calculation. From the HERA data on the ratio R^D [21, 22, 9] we obtain $C \simeq 1.5 \text{ GeV}^{-2}$.

In order to calculate multiparticle production in the chains of Fig. 4 we shall use the DPM-model [12] or QGSM-model [13] which give a good description of rapidity and multiplicity distributions in hadronic interactions. Thus we do not introduce any new free parameter in the calculation of multiparticle production in DIS.

In both models the hadronic spectra of each chain are obtained from a convolution of momentum distribution and fragmentation functions. The former are obtained from Regge intercepts [12] [13]. In the QGSM, used in the following calculations, the fragmentation functions into charged hadrons are given in ref. [25] with a normalization constant $a_h = 1.14$. The multiplicity distributions are computed assuming a Poisson distribution in clusters for the individual chains - with fixed rapidity positions of the chain ends. The formalism is described in detail in ref. [12]. The only parameter is the average charged multiplicity of the cluster decay, for which we use the same value $K = 1.4$ as in previous works. The weights for the configurations, with k -cut Pomerons ($2k$ -chains) are given by eq. (5). (A Monte Carlo code for multiparticle production in γp collisions, based on DPM, has been introduced by Engel and Ranft [26]).

It is important to note that our calculations are reliable only in the central

rapidity region and the proton fragmentation region, while the fragmentation region of the virtual photon can be dominated by perturbative production of jets of the type shown in Fig. 2. This region occupies an average rapidity $\sim \ell n \frac{Q^2}{m_{\perp h}^2}$, out of the total rapidity interval $\sim \ell n \frac{W^2}{m_{\perp h}^2}$. Unfortunately experiments at HERA cover mostly the photon fragmentation region and only a part of a central rapidity region. In the following comparison with experiment we will consider only the data in the central region of rapidity.

3 Comparison with experiment

Let us consider first the density of charged hadrons in the central rapidity region $\frac{dn^h(W^2, Q^2, y)}{dy} = \frac{1}{\sigma^{(tot)}(W^2, Q^2)} \frac{d\sigma^h(W^2, Q^2, y)}{dy}$. It is convenient also to consider the corresponding quantity for nondiffractive processes $\frac{dn_{ND}^h}{dy} = \frac{1}{\sigma^{ND}} \frac{d\sigma_{ND}^h}{dy}$, where $\sigma^{ND} \equiv \sigma^{(tot)} - \sigma^0 = \sum_{k=1}^{\infty} \sigma^k$. Due to AGK-cancellations [20] the inclusive cross section in the central rapidity region $\frac{d\sigma^h}{dy} \approx \frac{d\sigma_{ND}^h}{dy}$ is determined only by the contribution of the Pomeron pole and thus behaves as $\left(\frac{1}{x}\right)^\Delta$. For hadronic interactions, where rescattering effects for $\sigma^{(tot)}$ or σ^{ND} are very important, the increase of $\sigma^{(tot)}$ with energy is much slower and, as a result, $\frac{dn^h}{dy}$ (as well as $\frac{dn_{ND}^h}{dy}$) have a fast increase with energy. It was already emphasized in ref. [27] that in DIS $\sigma^{(tot)}$ and σ^{ND} have approximately the same $\left(\frac{1}{x}\right)^\Delta$ -behaviour as $\frac{d\sigma}{dy}$ (due to the small effect of the rescatterings) and $\frac{dn^h}{dy}$ should have weaker energy dependence than for hadronic interactions. Likewise, multiplicity distributions in DIS are expected to be narrower than in pp or γp and to show a much smaller KNO-scaling violation.

Predictions of the model for the mean charged multiplicity of nondiffractive events in the central pseudorapidity domains of DIS as functions of energy (W) are compared with H1-data [16] in Fig. 5a. Densities of particles in chains are taken from the model [13]. The DPM model leads to practically identical results. As explained above, the predictions of the model are most reliable for the smallest pseudorapidities ($1 < \eta^* < 2$), where they are in good agreement with experiment both in absolute magnitude and in the rate of increase with energy. In Fig. 5a we also show the results for the region $1 < \eta^* < 3$ where the agreement between theory and experiment, although still reasonable, is less good. It becomes slightly worse

when the size of the rapidity interval increases. Note that the agreement in the range $1 < \eta^* < 3$ is better at higher energies, where the distance between central rapidity region and fragmentation region of the virtual photon is larger. Model predictions for the rapidity distributions in DIS (for $Q^2 = 15 \text{ GeV}^2$) at different energies are shown in Fig. 5b. A substantial increase of the central plateau is predicted. At energies $W \lesssim 200 \text{ GeV}$ this increase is mainly connected with the increase of charged particle densities in the Pomeron chains. The faster increase at energies $\sqrt{W} > 10^3 \text{ GeV}$ is due to an increase of the average number of chains (cutted Pomerons). At these extremely high energies ($x \lesssim 10^{-5}$) effects of unitarization for structure functions are very important. Note, that as anticipated above, the energy rise of the central plateau in DIS is substantially smaller than the one measured in $\bar{p}p$ collisions.

The experimental data for charged hadrons produced in nondiffractive DIS in different pseudorapidity intervals of the central region [16] are compared with our predictions in Figs. 6. The agreement with experiment is good in the interval $1 < \eta^* < 2$ and becomes worse for larger intervals).

Comparison of theoretical predictions for different moments of multiplicity distributions with experimental data [16] is given in Table I. It is important to notice that the values of these moments are substantially smaller than the ones measured in $\bar{p}p$ scattering at the same energy (see Ref. [28]). This is a clear confirmation of the main feature of our approach, namely that the size of the rescattering contributions is smaller in DIS than in pp .

A further confirmation of this result could be obtained from the study of the energy dependence of the moments of the multiplicity distribution in DIS. It has been predicted in [29] that in the central rapidity interval $|y^*| < 1.5$, the moments C_i in $\bar{p}p$ should have a strong energy dependence. This dependence has been confirmed experimentally [28] (see also [12]). Such an energy dependence is due to the increase with energy of the fluctuations in the number of chains. Since the multi-chain (i.e. multi-cut Pomeron) contributions are smaller in DIS, we expect a smaller increase of the moments with energy. Note that models such as JETSET and MEPS based on perturbative QCD predict a magnitude and energy dependence of the DIS moments C_i in the central rapidity $1 < \eta^* < 2$, which is substantially different from our predictions [16].

Experimental studies of p_{\perp} -dependences of final hadrons at HERA [30, 31] are also in agreement with our assumption that in the central rapidity region ($y^* < 3$, for $W = 200$ GeV or $x_F < 0.07$) properties of final states are similar to the ones in γp or hp . Average transverse momenta in this region are much smaller than in the fragmentation region of the virtual photon [30].

Finally, let us now comment on multiparticle production in the virtual photon fragmentation region, where QCD perturbation theory can be applied. Though our model is strictly speaking not reliable in this region it still reproduces some features of multiplicity distributions up to pseudorapidity $\eta^* \sim 4$ though the agreement with experiment is worse than in the central rapidity region $\eta^* < 2 \div 3$. The model predicts very weak dependence of $\frac{dn}{d\eta^*}$ on Q^2 for fixed value of W and a rather strong dependence on W for fixed Q^2 . These consequences of the model are in an agreement with experimental results [16], which show that mean charged particle multiplicity is practically independent of Q^2 in the interval $10 \text{ GeV}^2 < Q^2 < 400 \text{ GeV}^2$ for fixed W . This observation is not easy to reconcile with predictions based on perturbative QCD, - radiation of extra gluons in the final state should lead to a substantial increase of multiplicity as Q^2 increases [32]. It may be an indication that the non-perturbative dynamics described above is important even in the fragmentation region of the virtual photon.

4 Conclusions

Our analysis indicates that production of hadrons in the central rapidity region in DIS can be understood in an approach based on the universality of the Pomeron. The model presented here does not contain any adjustable parameter. The size of the rescattering contribution has been determined from diffractive production data in DIS and all other parameters are fixed [12], [13] from high-energy hadronic interaction data. The model gives a quantitative description of the densities of charged particles in the central rapidity region and their multiplicity distributions at HERA energies. Possible tests of our approach in forthcoming experiments have also been presented.

Our results provide a clear confirmation of the idea, introduced in previous works

[9]-[10], that unitarity corrections, which play a capital role in pp interactions, are substantially smaller in DIS. Our model can provide a quantitative way of relating multiparticle production in hard and soft processes.

Acknowledgements

It is a pleasure to thank Yu. Dokshitzer, V. Khoze, G. Korchemsky, A. Krzywicki, G. Marchesini, A. Mueller and R. Peschanski for useful discussion.

This work was supported in part by grant INTAS 93-79 ext. and grant 96-02-19184 of the Russian Foundation for Fundamental Investigations.

Figure Captions

Fig. 1 :

The Pomeron-exchange diagrams for elastic γ^*p -scattering amplitude.

Fig. 2 :

Inelastic cuttings of the diagrams of Fig. 1. a) Totally inelastic final state.
b) Diffractive dissociation of a virtual photon.

Fig. 3 :

a) s -channel cutting of the single Pomeron exchange diagram of Fig. 1a).
b), c) Totally inelastic cuttings of the PP -exchange diagram of Fig. 1b).

Fig. 4 :

a) Two chains configuration corresponding to the diagram of Fig. 3a).
b) Production of 4-chains corresponding to the diagram of Fig. 3c).

Fig. 5 :

a) Comparison of theoretical predictions for energy dependence of mean charged multiplicity of nondiffractive events in central pseudorapidity domains of DIS with experimental data [16]. Lower points and curve correspond to $1 < \eta^* < 2$ and the upper ones to $1 < \eta^* < 3$.

b) Model predictions for the rapidity distributions of charged particles in the central rapidity region at various energies.

Fig. 6 :

Multiplicity distributions of charged hadrons produced in nondiffractive events in central pseudorapidity domains of DIS [16] compared to theoretical predictions.

a) $W = 97$ GeV, $1 < \eta^* < 2$; b) $W = 202$ GeV, $1 < \eta^* < 2$; c) $W = 97$ GeV, $1 < \eta^* < 3$; d) $W = 202$ GeV, $1 < \eta^* < 3$.

Table Caption

Table 1 :

Model predictions for various moments and cumulants of the multiplicity distributions of charged particles in DIS in two central pseudorapidity intervals and at two different energies are compared with H1 data [16].

References

- [1] M. Derrick et al (ZEUS Collaboration), Phys; Lett. **B293**, 465 (1992) ; **B316**, 41 (1993).
- [2] T. Ahmed et al (H1 Collaboration), Phys. Lett. **B299**, 85 (1992) ; I. Abt et al (H1), Nucl. Phys. **B407**, 515 (1993).
- [3] V. S. Fadin, E. A. Kuraev and L. N. Lipatov, Phys. Lett. **B60**, 50 (1975) ; Sov. Phys. JETP **45**, 199 (1977) ; I. I. Balitsky and L. N. Lipatov, Sov. J. Nucl. Phys. **28**, 822 (1978).
- [4] N. N. Nikolaev, B. G. Zakharov, J. Exp. Theor. Phys. **78**, 598 (1994) ; Phys. Lett. **B327**, 149, 157 (1994) ; N. N. Nikolaev, B. G. Zakharov and V. R. Zoller, J. Exp. Theor. Phys. **78**, 806 (1994) ; Phys. Lett. **B328**, 486 (1994) ; A. Mueller and H. Patel, Nucl. Phys. **B425**, 471 (1994).
- [5] M. Gluck, E. Reya and A. Vogt, Z. Phys. **C53**, 127 (1992).
- [6] A. D. Martin, R. G. Roberts and W. J. Stirling, Phys. Rev. **D50**, 6734 (1994).
- [7] H. L. Lai et al (CTEQ Collaboration), Phys. Rev. **D51**, 4763 (1996).
- [8] R. D. Ball and S. Forte, Phys. Lett. **B335**, 77 (1994) ; **B336**, 77 (1994).
- [9] A. Capella, A. Kaidalov, C. Merino and J. Tran Thanh Van, Phys. Lett. **B337**, 358 (1994).
- [10] A. Capella, A. Kaidalov, C. Merino and J. Tran Thanh Van, Phys. Lett. **B343**, 403 (1995) ; A. Capella, A. Kaidalov, C. Merino, D. Pertermann and J. Tran Thanh Van, Phys. Rev. **D53**, 2309 (1996).
- [11] V. N. Gribov, Zh. Eksp. Teor. Fiz. **57**, 654 (1967).
- [12] A. Capella, U. Sukhatme, C.-I. Tan and J. Tran Thanh Van, Phys. Rep. **236**, 225 (1994).
- [13] A. Kaidalov, in QCD at 200 TeV, eds. L. Cifarelli and Yu. Dokshitzer (Plenum, New York, 1992) p. 1.

- [14] A. Donnachie and P. V. Landshoff, Nucl. Phys. **B244**, 332 (1984) ; **B267**, 690 (1986).
- [15] A. Capella and A. Krzywicki, Phys. Rev. **D18**, 4120 (1978) ; A. Kaidalov, Proc. of XXII Intern. Conf. on Multiparticle Dynamics, ed. by C. Pajares, p. 185 (1992) ;
- [16] S. Aid et al (H1 Collaboration), DESY 96-160.
- [17] A. Kaidalov, Surveys in High Energy Physics **9**, 143 (1996).
- [18] J. D. Bjorken and J. Kogut, Phys. Rev. **D8**, 1341 (1973) ; J. D. Bjorken, SLAC-PUB-7096.
- [19] W. Büchmuller, Phys. Lett. **B353**, 335 (1995) ; W. Buchmuller and A. Hebecker, Phys. Lett. **355**, 573 (1995) ; Nucl. Phys. **B476**, 203 (1996).
- [20] V. Abramovskii, V. N. Gribov and O. V. Kancheli, Sov. J. Nucl. Phys. **18**, 308 (1974).
- [21] M. Derrick et al (Zeus Collaboration), Phys. Lett. **315**, 481 (1993) ; **B332**, 228 (1994) ; **B338**, 477 (1994) ; Z. Phys. **C70**, 391 (1996).
- [22] T. Ahmed et al (H1 Collaboration), Nucl. Phys. **B429**, 477 (1994) ; Phys. Lett. **B348**, 681 (1995).
- [23] K. A. Ter-Martirosyan, Nucl. Phys. **B36**, 566 (1972).
- [24] K. A. Ter-Martirosyan, Phys. Lett. **44B**, 377 (1973).
- [25] A. Kaidalov, Yad. Fiz. **45**, 1452 (1987).
- [26] R. Engel, Z. Phys. **C66**, 203 (1995) ; R. Engels and J. Ranft, ENSLAPP-A-540/95 (hep-ph/9509373).
- [27] A. Kaidalov, Proc. of the Workshop on the Leading Particle Effect, Erice, October (1996).
- [28] UA5 collaboration, R. E. Ansorge et al., Z. Phys. **C43**, 357 (1989).

- [29] A. Capella, A. Staar and J. Tran Thanh Van, Phys. Rev. **D32**, 2933 (1985) ;
A. Capella and J. Tran Thanh Van, Z. Phys. **C23**, 165 (1984).
- [30] I. Abt et al (H1 Collaboration), Z. Phys. **C63**, 377 (1994).
- [31] M. Derrick et al (Zeus Collaboration), Z. Phys. **C70**, 1 (1996).
- [32] L. V. Gribov, Yu. L. Dokshitzer, V. A. Khoze and S. I. Troyan, JETP Lett. **45**,
515 (1987) ; Sov. Phys. JETP **67**, 1303 (1988) ; Phys. Lett. **B202**, 276 (1988).

	$\langle W \rangle = 201.9$			
	$1 < \eta^* < 2$	$1 < \eta^* < 2$	$1 < \eta^* < 3$	$1 < \eta^* < 3$
C_2	1.69	$1.69 \pm 0.02 \pm 0.03$	1.48	$1.44 \pm 0.01 \pm 0.02$
C_3	3.81	$3.75 \pm 0.12 \pm 0.20$	2.83	$2.62 \pm 0.09 \pm 0.09$
C_4	10.73	$10.02 \pm 0.65 \pm 1.22$	6.68	$5.71 \pm 0.47 \pm 0.34$
R_2	1.34	$1.32 \pm 0.02 \pm 0.03$	1.29	$1.26 \pm 0.01 \pm 0.03$
R_3	2.26	$2.11 \pm 0.09 \pm 0.13$	2.06	$1.88 \pm 0.08 \pm 0.11$
K_3	0.255	$0.147 \pm 0.043 \pm 0.101$	0.204	$0.108 \pm 0.041 \pm 0.036$
	$\langle W \rangle = 96.9$			
	$1 < \eta^* < 2$	$1 < \eta^* < 2$	$1 < \eta^* < 3$	$1 < \eta^* < 3$
C_2	1.71	$1.71 \pm 0.02 \pm 0.02$	1.48	$1.40 \pm 0.01 \pm 0.03$
C_3	3.85	$3.87 \pm 0.16 \pm 0.18$	2.78	$2.41 \pm 0.04 \pm 0.16$
C_4	10.72	$10.67 \pm 0.93 \pm 1.23$	6.38	$4.83 \pm 0.19 \pm 0.64$
R_2	1.31	$1.30 \pm 0.02 \pm 0.03$	1.26	$1.19 \pm 0.01 \pm 0.03$
R_3	2.11	$2.11 \pm 0.14 \pm 0.15$	1.91	$1.64 \pm 0.04 \pm 0.13$
K_3	0.139	$0.187 \pm 0.070 \pm 0.097$	0.139	$0.048 \pm 0.015 \pm 0.044$

Table 1

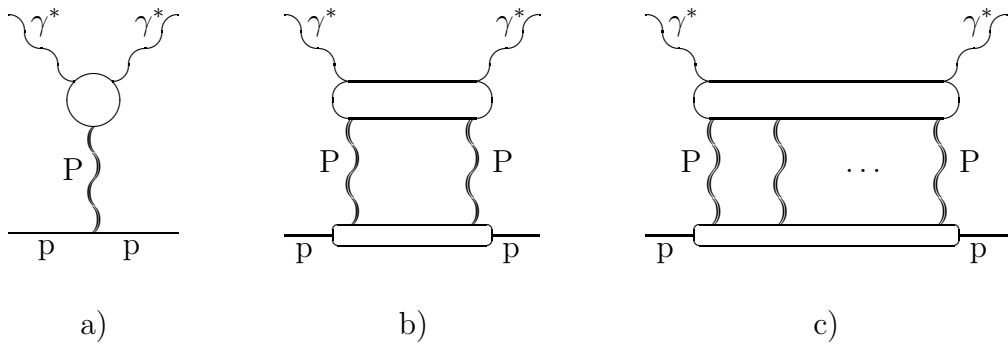


Fig. 1

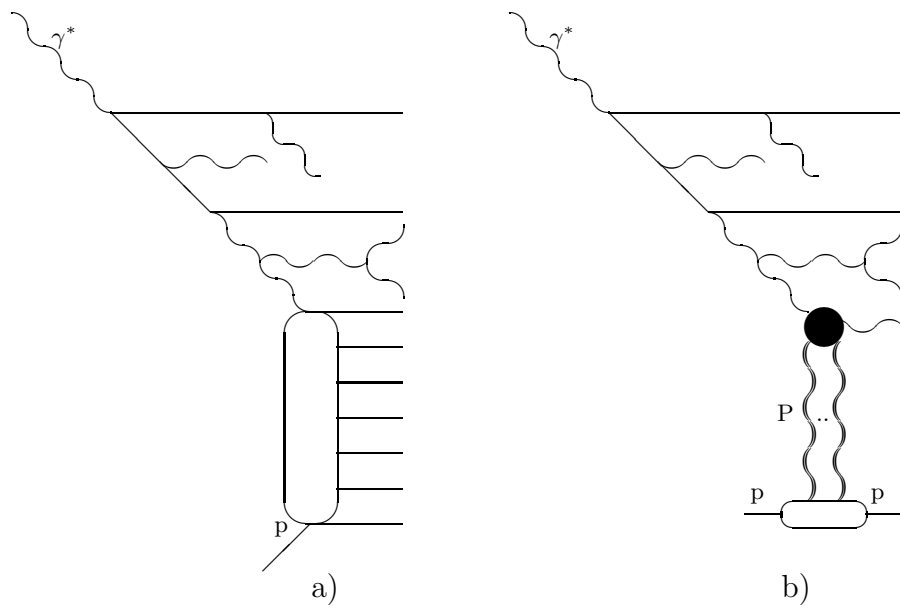
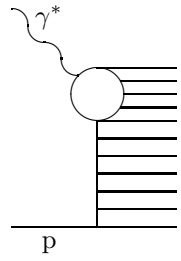
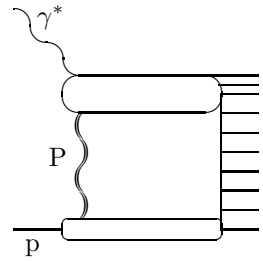


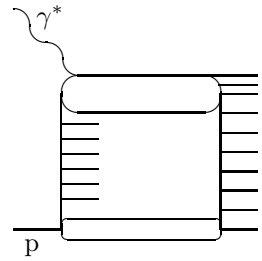
Fig.2



a)



b)



c)

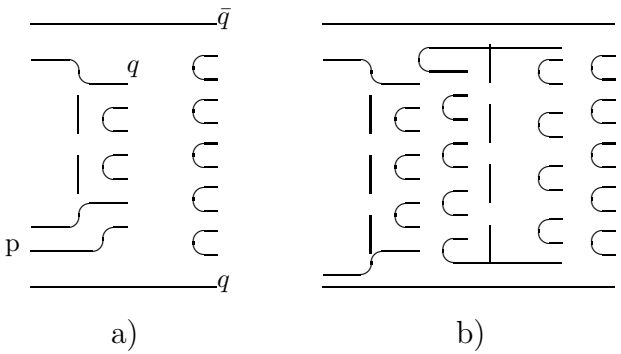


Fig.4

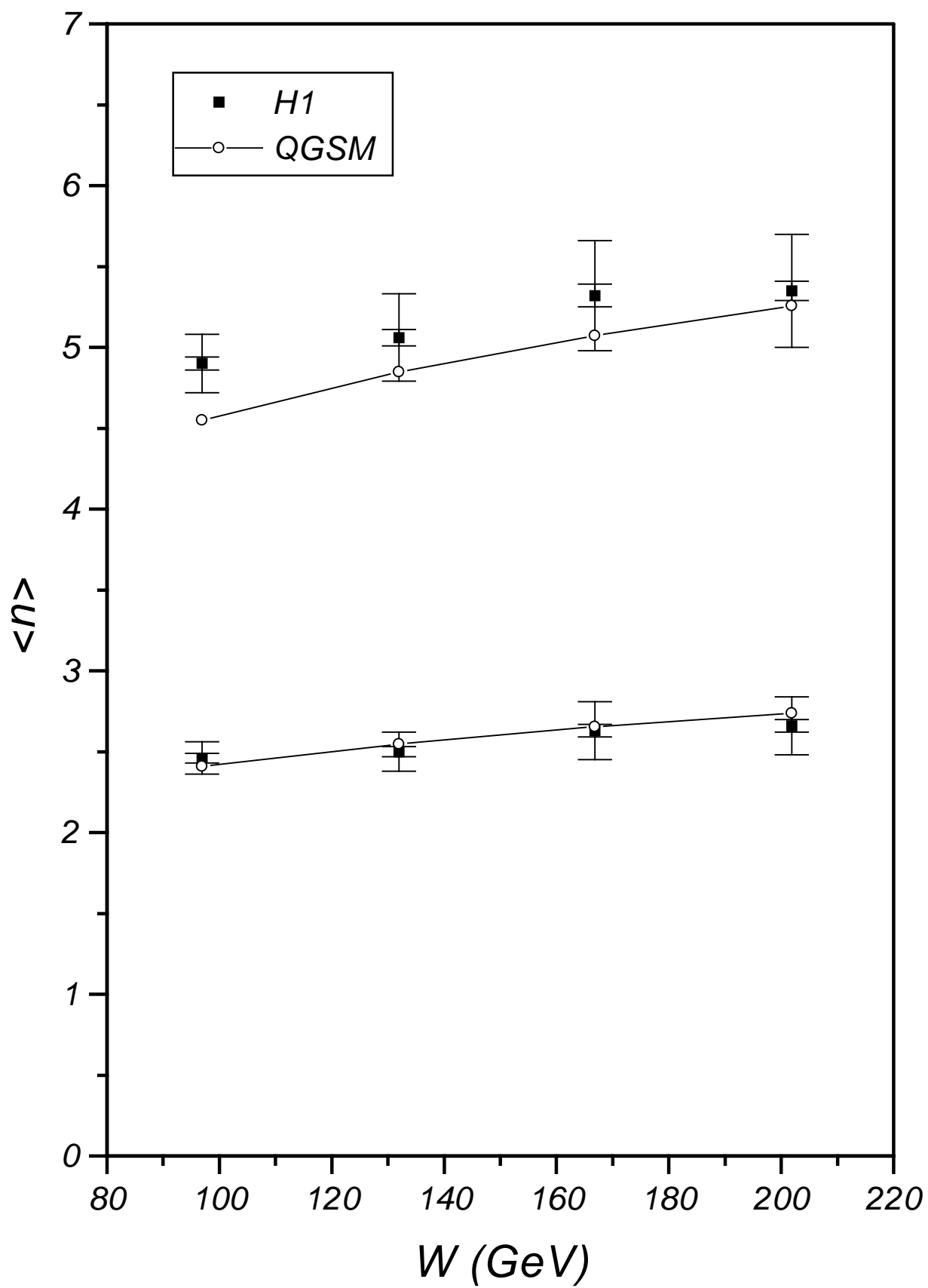


Fig. 5a

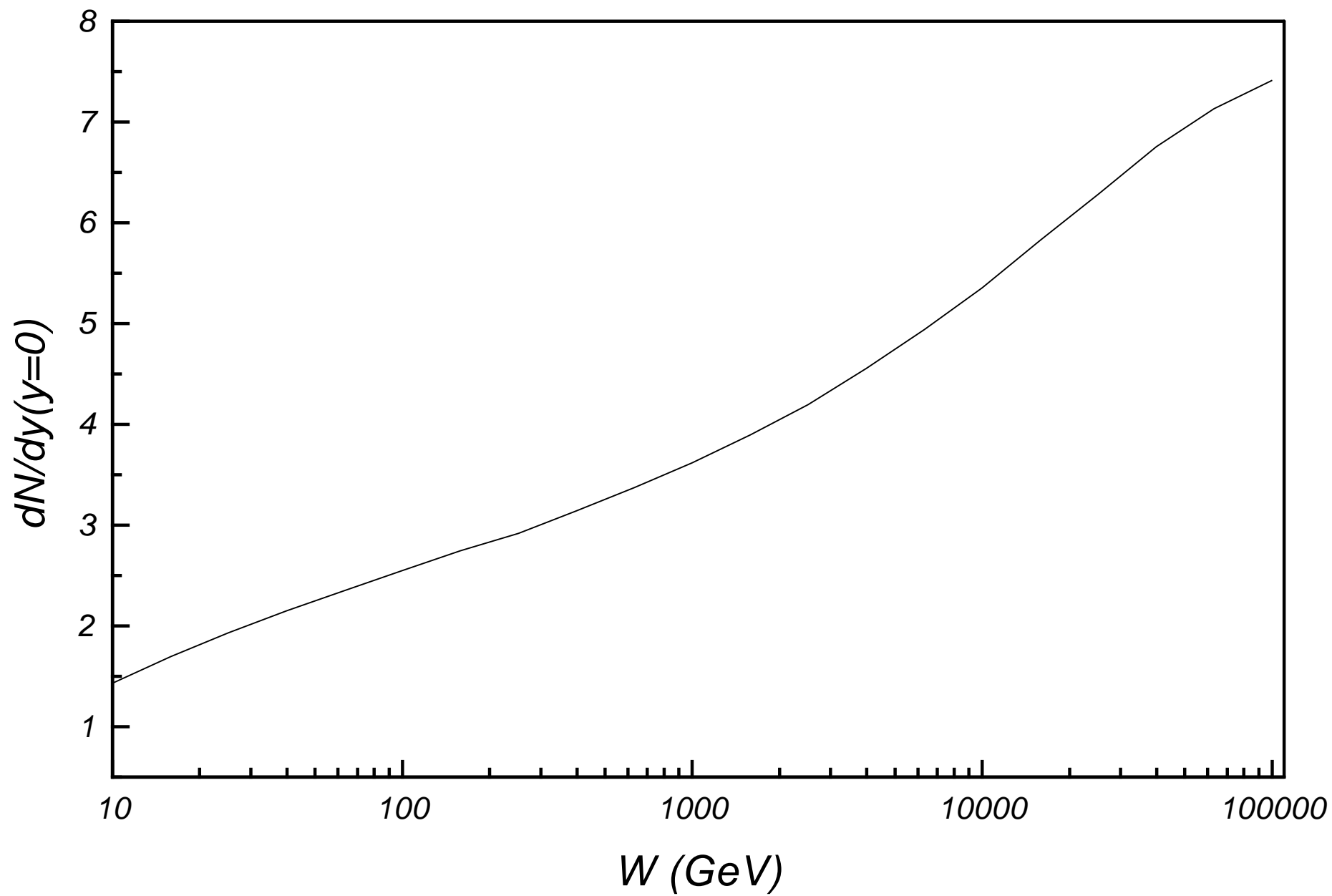


Fig. 5b

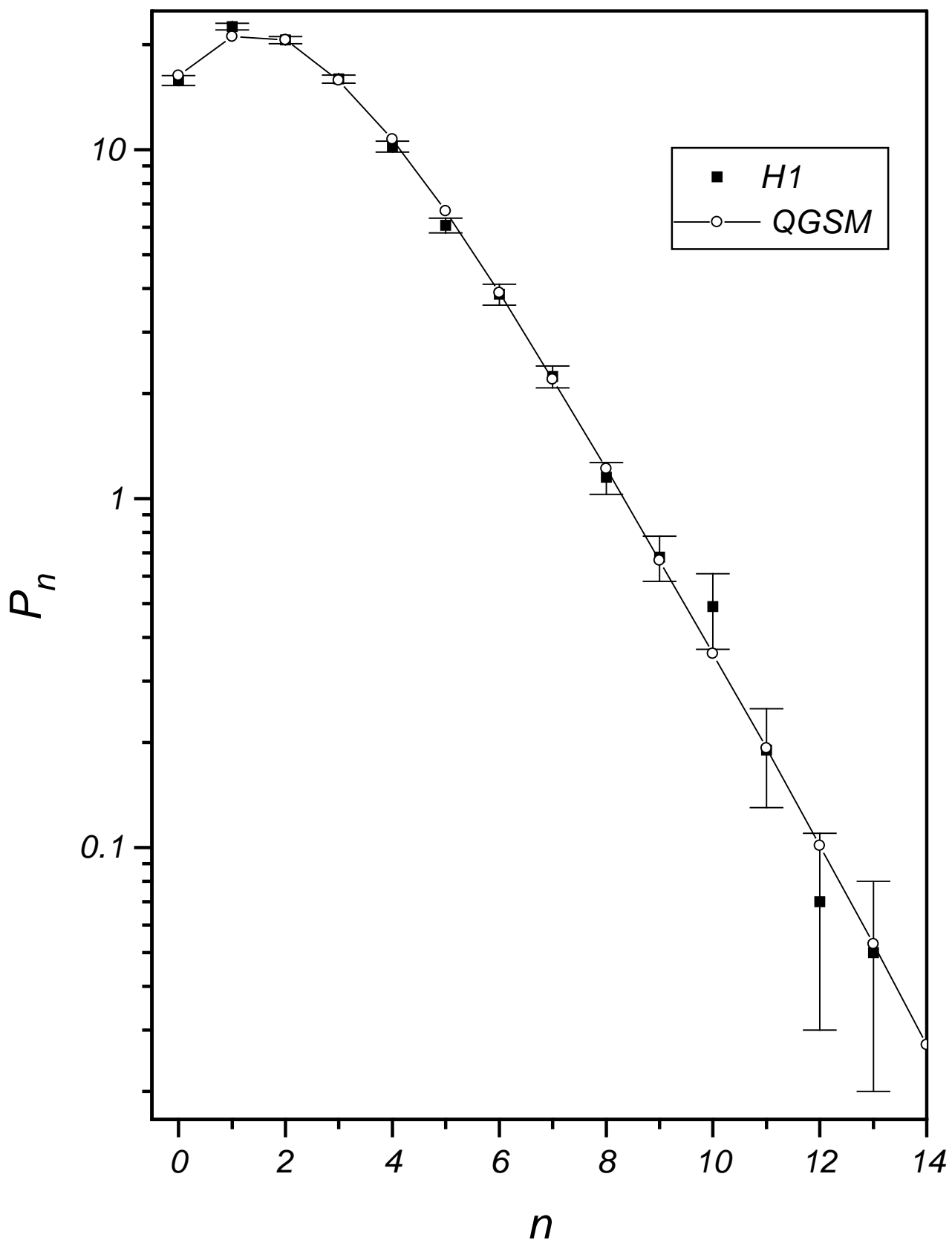


Fig. 6a

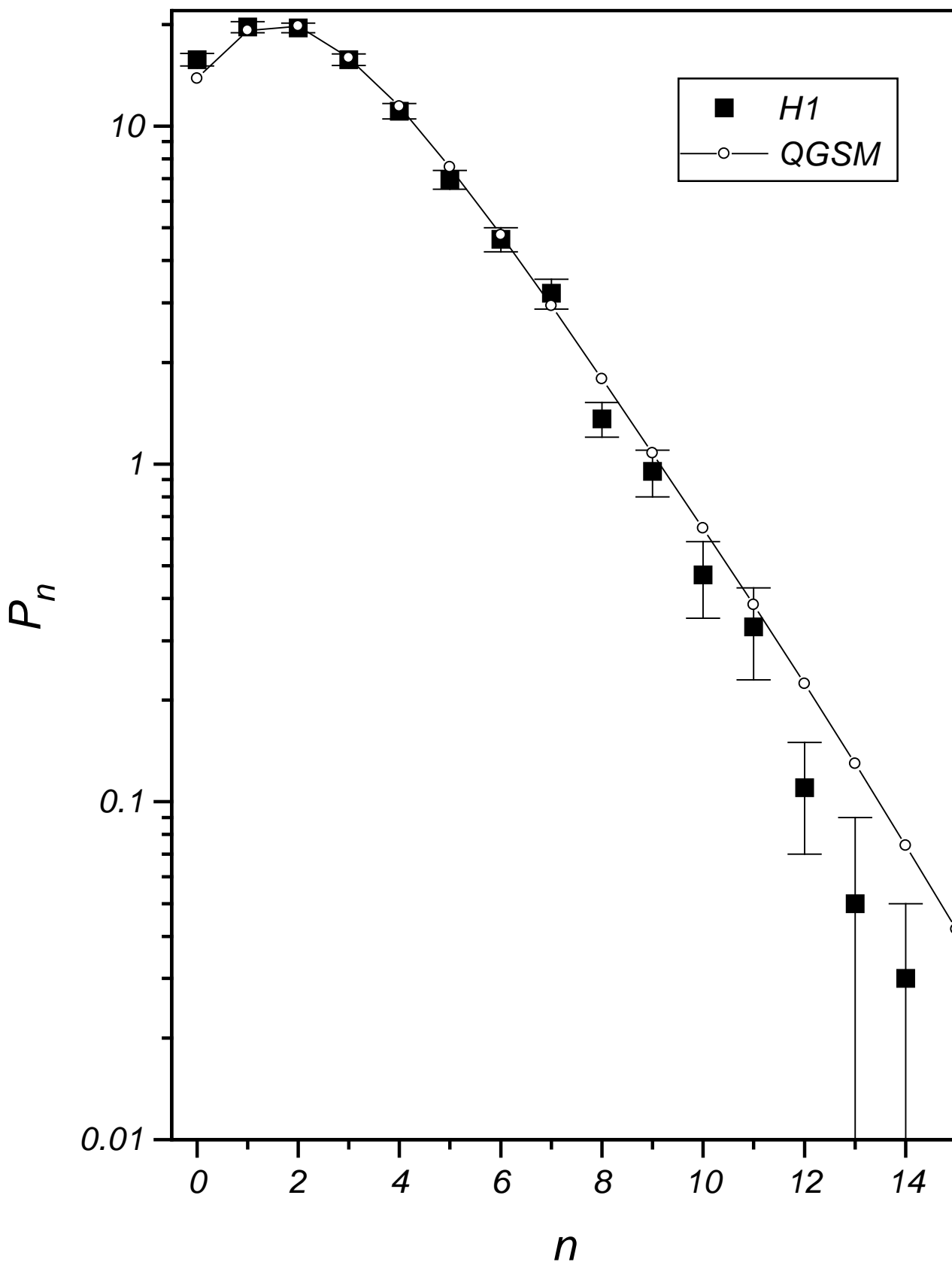


Fig. 6b

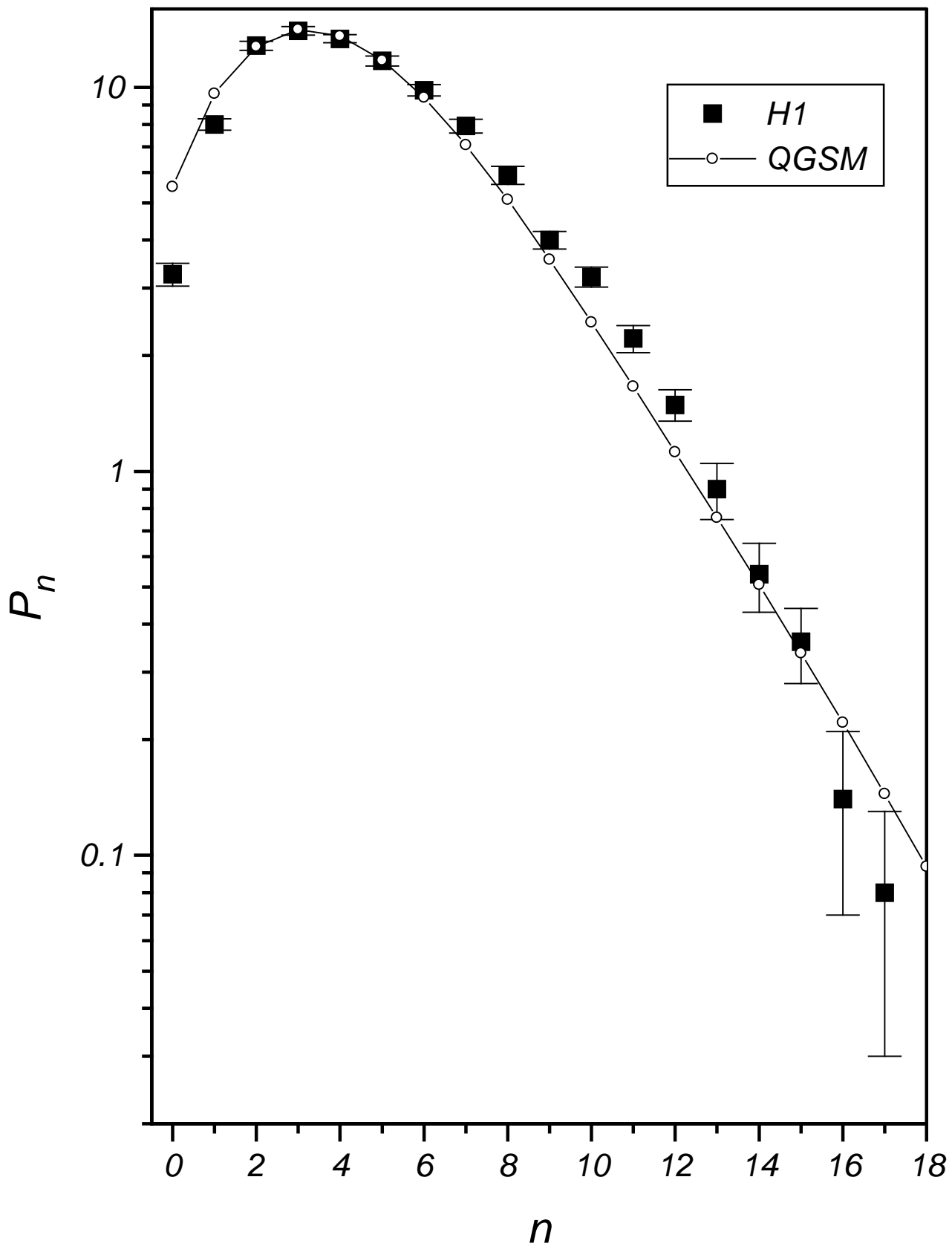


Fig. 6c

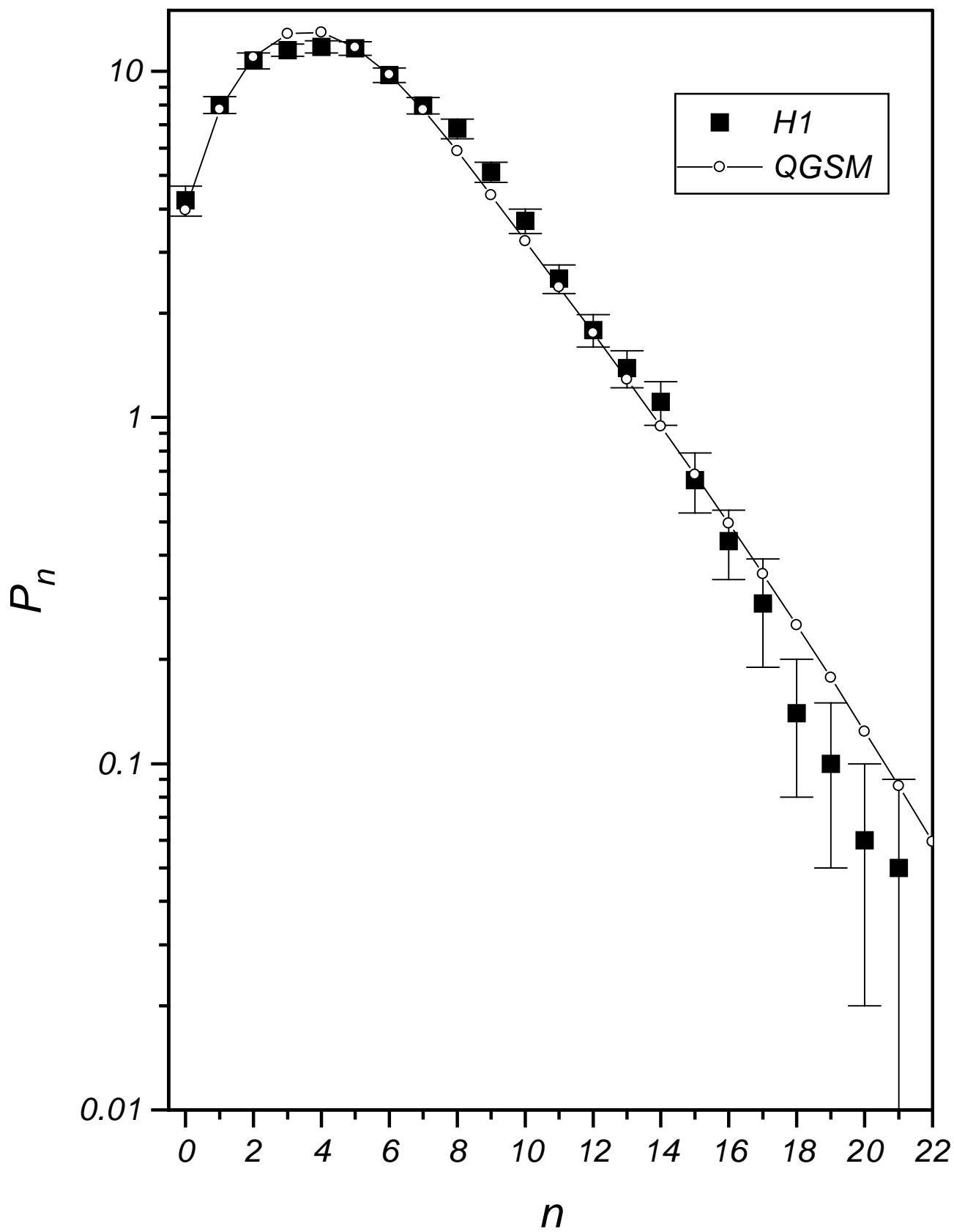


Fig. 6d